A Journal of the Gesellschaft Deutscher Chemiker

Angewandte International Edition GDCh Chemie

www.angewandte.org

Accepted Article

Title: Redox-active hybrid polyoxometalate-stabilised Au nanoparticles

Authors: Carmen Martin, Katharina Kastner, Jamie M Cameron, Elizabeth Hampson, Jesum Alves Fernandes, Emma K Gibson, Darren A Walsh, Victor Sans, and Graham N. Newton

To be cited as: *Angew. Chem. Int. Ed.* 10.1002/anie.202005629

Link to VoR: https://doi.org/10.1002/anie.202005629

WILEY-VCH

10.1002/anie.202005629

WILEY-VCH

COMMUNICATION

Redox-active hybrid polyoxometalate-stabilised Au nanoparticles

Carmen Martin,[a,b] Katharina Kastner,[a] Jamie M. Cameron,[a] Elizabeth Hampson,[a] Jesum Alves Fernandes,[c] Emma K. Gibson,[d] Darren A. Walsh,[a]* Victor Sans,[a,e]* and Graham N. Newton[a]*

Abstract: We report the design and preparation of multifunctional hybrid nanomaterials through the stabilization of gold nanoparticles with thiol-functionalised hybrid organic-inorganic polyoxometalates. The covalent attachment of the hybrid-POM forms new nanocomposites which are stable at temperatures and pH values, which destroy analogous electrostatically-functionalised nanocomposites. Photoelectrochemical analyses reveal the unique photochemical and redox properties of these systems.

Due to their unique catalytic, electronic and optical properties, gold nanoparticles (AuNPs) are used in a wide range of areas, including healthcare, sensing, catalysis, and photonics.[1] To prevent agglomeration of AuNPs during nucleation and growth, a range of surfactants and capping agents are often used in their synthesis. These capping agents can also be designed to impart added functionality, such as redox activity.[2] In this regard, the use of redox-active polyoxometalates (POMs) offers a range of material-design opportunities owing to their stability and enormous structural and compositional diversity. POMs are anionic metal oxide clusters that exhibit rich electrochemical and photochemical properties,[3] and are increasingly-popular reducing agents[4] and electrostatic capping agents[5] for the synthesis of metal NPs and nanocomposites.[6]

In parallel to the development of NP@POM composites, the past decade has seen a rapid increase in the development of organic/inorganic hybrid-POMs, in which organic groups are covalently tethered to the metal oxide cluster.[7] The properties of such materials can be finely tuned by changing the nature of the POM and the organic modifier,[8] paving the way for the rational molecular design of new multifunctional supramolecular materials.[7,9] For instance, it was recently shown that POMs could be functionalised with organophosphoryl groups to prepare a new family of amphiphilic hybrid POM surfactants.[10] The surfactant molecules self-assemble in solution to form micellar aggregates that retain the (modified) redox properties of the molecular building blocks and similar nanoscale systems have been proposed as charge carriers for use in solution-phase energy-storage systems.[11] Hybrid POMs have also been used as capping agents for Au NPs,[12] where thiol-terminated organosilane functionalised clusters are used to covalently stabilise the NP surface. This strategy is notable in that it minimises desorption of the POM capping groups and presents additional opportunities for synthetic control over the system. For instance, Polarz et al. have recently shown how synergistic interactions between appended hybrid-POM and the surface-plasmon resonance of AuNPs can enhance photocatalytic activity.[13] Whilst these studies point to the considerable promise of such materials, our understanding of the stability and emergent properties of these systems remains very much in its infancy, limiting our ability to rationally prepare new nanomaterials with properties tailored towards specific, novel applications.

Here, we describe the synthesis and properties of AuNPs stabilised by a thiol-bearing hybrid organophosphoryl-modified Wells-Dawson POM, $K_6[P_2W_{17}O_{61}(PO_2C_{17}H_{26}\text{-}SH)_2]$ (**1**),[14] and report a detailed comparison of the new Au@hybrid-POM nanoparticle composite (**NP-1**) with its electrostatically-stabilised analogue (**NP-P_2W_{18}**), comprising AuNPs non-covalently capped with the conventional $K_6[P_2W_{18}O_{62}]$ (**{P_2W_{18}}**) Wells-Dawson cluster.[15] Transmission electron microscopy (TEM), X-ray photoelectron spectroscopy (XPS), X-ray absorption near-edge structure (XANES), UV-visible absorption, and FT-IR analyses have been used to probe the structure and surface interactions of both nanoparticle composites, whilst spectroscopic and voltammetric analyses have been used to compare their photo-- and electro-chemical properties, respectively. As such, this represents the first detailed analysis of the vital role played by direct chemical attachment of the multi-functional POM capping agent to the nanoparticle surface.

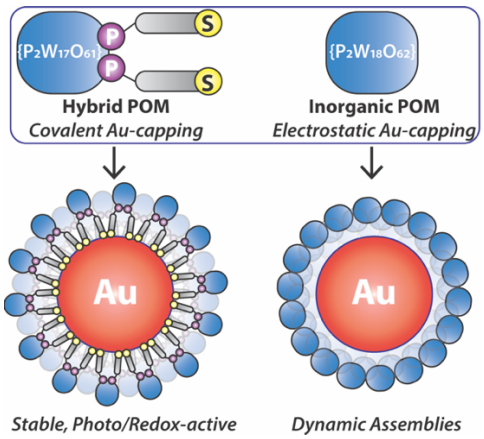

Scheme 1. A route to stable, redox and photo-active NP@POM composites.

[a] Dr. C. Martin, Dr. K. Kastner, Dr. J. M. Cameron, E. Hampson, Dr. Dr. D. A. Walsh, and Dr. G N. Newton
Nottingham Applied Materials and Interfaces (NAMI) Group,
The GSK Carbon Neutral Laboratories for Sustainable Chemistry,
University of Nottingham, Nottingham, NG7 2TU, UK
E-mail: graham.newton@nottingham.ac.uk
darren.walsh@nottingham.ac.uk
[b] Dr Carmen Martin
Universidad de Sevilla, Departamento de Quimica Fisica, Facultad de Quimica, 41012 Sevilla, Spain
[c] Dr. J. Alves Fernandes
School of Chemistry, University of Nottingham.
University Park, Nottingham, NG7 2RD, UK
[d] Dr. E. K. Gibson
School of Chemistry, University of Glasgow,
Glasgow, G12 8QQ, UK
[e] Dr. V. Sans
Institute of Advanced Materials (INAM)
University Jaume I, 12006 Castellon, Spain
E-mail: sans@uji.es

Supporting information for this article is given via a link at the end of the document.

10.1002/anie.202005629

WILEY-VCH

COMMUNICATION

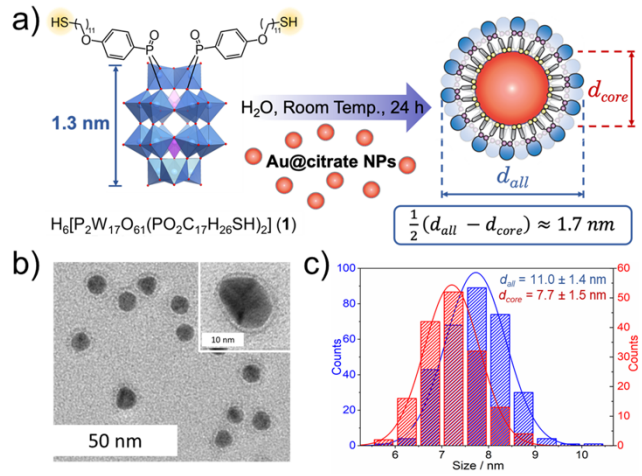

Figure 1. a) Schematic showing the synthesis of **NP-1** (colour code: {WO_6} = blue polyhedra; {PO_4} = purple polyhedra; Au nanoparticles = red spheres; hybrid-POM **1** = blue spheres, cations omitted for clarity); b) TEM micrograph of **NP-1** highlighting the surface-bound monolayer of POMs (inset); c) size distributions for **NP-1** determined by TEM analysis.

The synthesis of the hybrid-POM capping ligand, **1**, was carried out using a modified version of the synthesis previously described by our group.[14] Briefly, 4-((11-(thio)undecyl)-oxy) phenyl-phosphonic acid and the mono-lacunary precursor $K_{10}[P_2W_{17}O_{61}]$ were combined *via* an acid-mediated condensation reaction in acetonitrile (see Supporting Information). The hybrid-Au@POM composite **NP-1** was then synthesised by mixing **1** with a solution of 10 nm citrate-stabilised Au NPs (**Au@citrate**) in H_2O and stirring for 2 days at room temperature. The resulting composite nanoparticles had an Au-to-W ratio of 34:1 and the average number of POMs per Au NP was found to be *ca.* 400 (according to inductively-coupled plasma optical emission spectroscopy – refer to Section 8 in the SI). **NP-P_2W_{18}** was synthesised according to the same method, but using **{P_2W_{18}}** in place of **1**.

TEM of both nanocomposites showed that **NP-1** comprised monodisperse and well-separated NPs with an average diameter (d_{all}) of 11.0 nm (Figure 1) Owing to the excellent contrast of W in TEM imaging, a clear surface layer of POMs could be resolved as a ring around the surface of the AuNPs in **NP-1**. This layer is estimated to have a thickness of 1.7 nm, corresponding closely to the expected dimensions of a monolayer of hybrid-POM clusters.

No such effect was observed for **NP-P_2W_{18}**, where agglomerated groups of NPs (d = 7.2 nm) with a similar shape to the Au@citrate nanoparticle precursors were observed (Figure S22-24). This suggests that weaker or unstable coverage of the nanoparticle surface resulted when te electrostatic capping approach was used (agreeing with the aggregation observed in TEM imaging of these materials).

FTIR spectroscopy of **NP-1** showed similar features to that of the hybrid-POM **1**, while **NP-P_2W_{18}** more closely resembles those of citrate-capped Au NPs (Figures S11 and S12).[16] This can be attributed to the excellent surface coverage of **1** on the Au NPs (see SI). The UV-visible spectrum of **NP-1** also exhibits features consistent with successful formation of the nanocomposite: a strong absorption centred at 335 nm corresponding to the ligand-to-metal charge transfer (LMCT) band of the hybrid-POM and a surface-plasmon resonance (SPR) peak at 531 nm (Figure S15).[17] The SPR peak is centred at a slightly longer wavelength than that of the citrate-stabilised Au NP precursors (527 nm) which is due to the different refractive indices of the capping agents, confirming the successful capping of the Au NPs with **1**. The SPR peak of **NP-P_2W_{18}** was found to be broader than that of the citrate-capped NPs and was red-shifted by about 15 nm (Figure S18), consistent with agglomeration of the NPs as revealed previously by TEM.

The stability of both composites was compared against a range of different conditions. The thermal stability of both materials was studied *via* UV-vis spectroscopic analysis. Where the plasmon resonance band of **NP-1** showed no change after heating at 80 °C for 24h, that of **NP-P_2W_{18}** disappeared (Figures S32 and S33). Furthermore, **NP-1** was stable upon storage for 1 month at –6 °C, and for at least 24h in both 0.5 % H_2O_2 and buffer solutions (pH 5 and 7; measured at 37 °C). Conversely, **NP-P_2W_{18}** degraded under all of these conditions (Figures S34-S38). The excellent stability of **NP-1** in a range of environments (including under biologically relevant conditions) suggests that **NP-1** and similar covalently-stabilised NP@POM materials could find use in a range of potentially demanding applications such as sensing or catalysis.

Following basic characterisation and comparison of our systems, we probed the interactions between the capping POM groups and nanoparticle surfaces. XPS was performed as a means to investigate the Au-POM interaction in both systems (Figure 2a). The Au 4f core XPS spectrum of **NP-P_2W_{18}** shows significantly lower binding energies (83.3 and 87.00 eV) when compared to **NP-1** (84.0 and 87.7 eV). This is further evidence

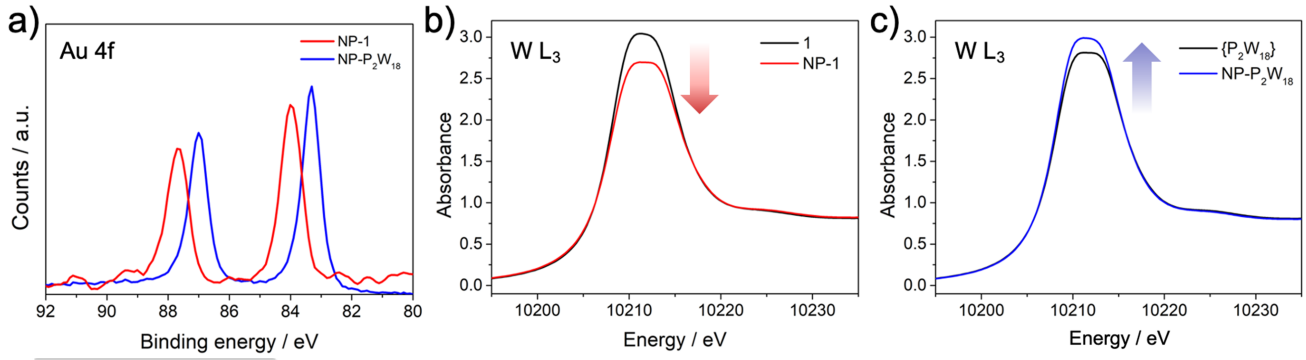

Figure 2. a) XPS spectra of **NP-1** and **NP-P_2W_{18}** showing the Au $4f_{7/5}$ and $4f_{7/2}$ absorptions, respectively; b) XANES spectra of the hybrid POM **1** compared to the nanocomposite **NP-1**, showing a decrease in the intensity of the W L_3 'white line' absorption edge upon formation of the hybrid nanomaterial, and; c) XANES spectra of **{P_2W_{18}}** compared to **NP-P_2W_{18}**, showing an increase in the intensity of the W L_3 absorption edge upon interaction of the POMs with Au.

10.1002/anie.202005629

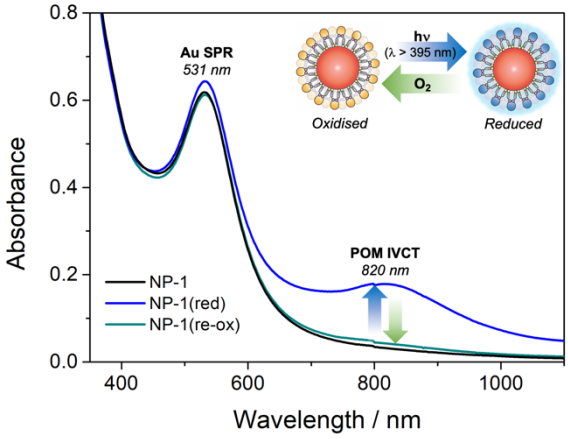

Figure 3. UV-Vis absorption spectra of **NP-1** in DMF showing spectrum after photoreduction of capping POMs with visible light (blue) and after subsequent aerobic oxidation and recovery of the native state (green).

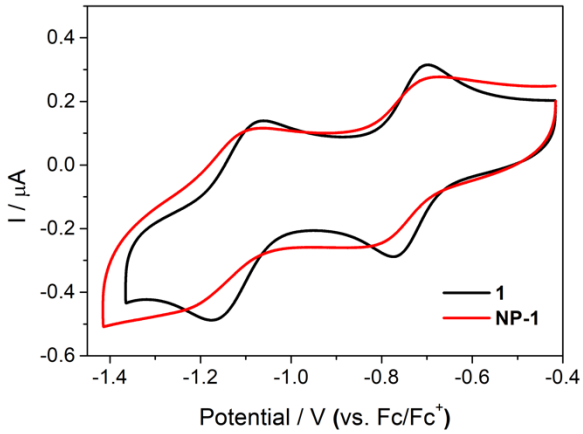

Figure 4. Cyclic voltammograms of 0.125 mM solutions of **1** and **NP-1** in DMF at a scan rate of 100 mV s^{-1}. Initial scan was to negative potentials. Potentials have been reported relative to that of the Fc/Fc^+ redox couple.

that the capping agents in **NP-P_2W_{18}** have a strong electrostatic interaction with the Au surface, and similar binding energies were also recently found by Weinstock *et al.* for analogous electrostatically-decorated Au@{P_2W_{18}} NPs (83.5 and 87.20 eV).[6d] Typically, lower binding energies point towards decreased oxidation states or, more accurately in this case, a higher negative surface polarisation/charge density resulting from the capping of the Au NPs by the negatively charged POM in **NP-P_2W_{18}**.[6d,18] It is therefore interesting that the binding energies found in **NP-1** are comparatively higher and, in fact, are an excellent match to the values expected for both thiol-functionalised Au^0 surfaces,[19] and bulk Au^0 (84.0 and 87.70 ± 0.2 eV). This suggests that the POM clusters are shielded from the Au surface by the ligand groups which helps to minimise the electrostatic interaction between them. A similar effect has been previously reported by Cronin and Kadodwala *et al*. for POM monolayers on gold surfaces.[20]

To further probe the surface interactions of the POM-capped nanomaterials, XANES analysis was performed on both **NP-1** and **NP-P_2W_{18}** and compared to the corresponding spectra for the native POM cluster in each case (Figure 2b-c). The broad 'white line' W-L_3-edge observed in all four spectra corresponds well to the expected peak shape for distorted {WO_6} octahedra.[21] More interestingly, the intensity of the white line signal can also provide an indication of the charge density associated with the W-centres. Here, a clear difference can be observed between the covalently-bound species in **NP-1** and the electrostatically-bound clusters in **NP-P_2W_{18}**. The white line intensity falls in the case of the former, suggesting an increase in the effective charge density of the W centres in the hybrid-POM, whereas it rises in the case of the latter, suggesting a reduction in the charge density. This supports the findings of the XPS analysis, suggesting that each POM interacts differently with the Au surface. In the case of the non-covalent composites, **{P_2W_{18}}** donates electron density in a manner similar to that previously discussed by Weinstock.[6d] As discussed above however, the covalently-bound POMs in **NP-1** are effectively shielded from the gold surface and do not electronically interact with it. Instead, one possibility is that the tight-packing of the POM monolayer around the NPs (which have a notably high POM-loading) increases the coulombic interactions between neighbouring anions, significantly modifying the local environment of each cluster. This agrees with previous observations we have made on micellar systems,[14] and also with previous studies of POM monolayers formed on Au NPs, where even the extensive integration of counter-cations into the monolayer does not fully attenuate the high negative charge at the composite surface.[6c] This is likely to have profound implications for the photochemical and redox properties of the composite materials (*vide infra*).

The photochemical properties of the new nanocomposites were evaluated by irradiating a de-aerated sample of **NP-1** in *N*,*N*'-dimethylformamide (DMF) using a solar simulator (200 W) fitted with a 395 nm cut-off filter. After a 30 minutes of visible-light irradiation, the absorption spectrum of **NP-1** exhibited the typical intervalence charge transfer (IVCT) band expected for a mono-reduced organophosphoryl hybrid Wells-Dawson ion at 820 nm,[8a] while the SPR band from the Au NP core at 531 nm remained intact (Figure 3). Interestingly, the sample could be easily and cleanly re-oxidised by bubbling O_2 into the solution, and several reduction-oxidation cycles could be performed without any evidence of decomposition (Figure S30), indicating that these materials may be useful for photometric or photocatalytic applications.[22] In contrast, the photoreduced state of **NP-P_2W_{18}** could only be accessed using harder UV irradiation (*i.e.* < 395 nm), under which conditions **NP-P_2W_{18}** decomposed (Figure S31). Whilst organophosphonate hybrid-POM clusters in particular are known to be photoactive in the near-visible regime, their photoreduction can be difficult to reverse in O_2 due to their low lying LUMO levels and correspondingly more positive redox potentials.[23] One possibility is that the tightly packed structure of **1** on the NP surface may destabilise the reduced state of the POM, as seen previously in micellar systems,[14] facilitating its re-oxidation by a relatively mild oxidant (O_2).

Owing to the highly reversible, rich multi-electron redox chemistry conferred by the POM capping groups, we also studied the electrochemical properties of both composites. Cyclic voltammetry of 0.125 mM **NP-1** in DMF shows two quasi-reversible redox processes, centred at –0.76 V (peak to peak separation, ΔE_p = 90 mV) and –1.15 V (ΔE_p = 140 mV) vs. Fc/Fc^+. This cyclic voltammogram is similar to that of the discrete hybrid-POM **1** ($E_{1/2}$ = -0.74 V (ΔE_p = 70 mV) and -1.12 V (ΔE_p = 100 mV), see Figure 4). The larger ΔE_p values and negatively shifted redox potentials observed for **NP-1** indicates that reduction/oxidation is more kinetically and thermodynamically hindered in this system. This agrees with both the XANES analysis, which indicates that **1** is more electron-rich when bound to the NP surface (Fig. 2b), and

our previous discussion around the aerobic reoxidation of the photoreduced state. **NP-1** is also shown to be stable to repeated potential cycling (Figure S20), highlighting the strong attachment of the POM to the Au surface. In contrast, the behaviour of **NP-P_2W_{18}** is identical to that of the **{P_2W_{18}}** capping groups (Figure S19), indicating that the kinetics of electron transfer to and from the weakly bound POMs appear unaffected by their electrostatic association to the AuNP surface. The electrochemical properties of **1** and **NP-1** were also compared *via* voltammetry using a Pt ultramicroelectrode (see SI for details). **1** yielded a clear steady-state voltammogram due to efficient, convergent diffusion of the redox species to the electrode surface from the expanding diffusion field. In contrast, **NP-1** yielded a transient (peak-shaped) response due to depletion of the slowly-diffusing nanocomposite within the diffusion field next to the electrode surface, consistent with the retention of stable POM-NP interactions in **NP-1.**

We have successfully prepared highly stable AuNPs functionalised with covalently-bound organic-inorganic hybrid POMs. Extensive characterization of the new nanomaterial (**NP-1**) was performed using a range of spectroscopic and imaging techniques, demonstrating unambiguously that hybrid POMs are directly attached to the Au NP surface through a thiolate-type binding mode. The thermal, chemical, photochemical and electrochemical stability of the new covalent nanocomposite was investigated through detailed comparison with an electrostatically functionalised analogue (**NP-P_2W_{18}**), clearly demonstrating the crucial and highly effective role that covalent functionalisation plays in stabilising the assembly. This multifunctional nanomaterial was found to combine the optical properties of gold nanoparticles with the electro- and photochemical features of POMs. The rich, reversible electrochemistry and remarkable, efficient and reversible photoactivation under visible light means that these materials may find new application in a range of catalytic and sensing technologies. Future work will explore how more systematic approaches to the molecular design of the hybrid POM, in conjunction with the nanoparticle size, shape and composition, can be used to both tailor and improve the properties of new composite materials.

Acknowledgements

The authors thank the University of Nottingham Propulsion Futures Beacon of Excellence. KK thanks the Deutscher Akademischer Austausch Dienst (DAAD). EH thanks the Low Dimensional Materials and Interfaces Doctoral Training Programme at the University of Nottingham. JC, VS and GN thank the Leverhulme Trust (RPG-2016-442). GN and DW thank the Centre of Advanced Materials for Integrated Energy Systems (CAM-IES). GN and VS thank the EPSRC Directed Assembly Network. VS thanks the Generalitat Valenciana (CIDEGENT/2018/036) for funding. The authors thank the Diamond Light Source for provision of beamtime (SP15151).

Conflict of interest.

The authors declare no conflict of interest

Keywords: redox chemistry • gold nanoparticle • hybrid material • photochemistry • polyoxometalate

[1] a) K. Saha, S. S. Agasti, C Kim, X. Li and V. M. Rotello, *Chem. Rev.* **2012,** *112*, 2739–2779; b) H. Kang, J. T. Buchman, R. S. Rodriguez, H. L. Ring, J. He , K. C. Bantz and C. L. Haynes, *Chem. Rev.* **2019**, *119*, 664–699; c) R. Ahmad, N. Griffete, A. Lamouri, N. Felidj, M. M. Chehimi and C. Mangeney, *Chem. Mater.* **2015**, *27*, 5464−5478; d) M. C. Daniel and D. Astruc, *Chem. Rev.* **2004**, *104*, 293−346; e) Y. Zhang, X. Cui, F. Shi and Y. Den. *Chem. Rev*. **2012**, *112*, 2467–2505.

[2] M.-C. Daniel, J. Ruiz, S. Nlate, J.-C. Blais and D. Astruc, *J. Am. Chem. Soc.* **2003**, *125*, 2617–2628.

[3] a) X. Lopez, J. J. Carbo, C. Bo and J. M. Poblet, *Chem. Soc. Rev.* **2012**, *41*, 7537-7571; b) J. J. Walsh, A. M. Bond, R. J. Forster and T. E. Keyes, *Coord. Chem. Rev.* **2016**, *306*, 217–234.

[4] A. Troupis, A. Hiskia and E. Papaconstantinou, *Angew. Chem. Int. Ed.* **2002**, *41*, 1911–1914.

[5] a) Y. Lin and R. G. Finke, *J. Am. Chem. Soc.* **1994**, *116*, 8335–8353 b) C. R. Graham, L. S. Ott and R. G. Finke, *Langmuir* **2009**, *25*, 1327–1336; c) S. Martín, Y. Takashima, C.-G. Lin, Y.-F. Song, H. N. Miras and L. Cronin, *Inorg. Chem.* **2019**, *58*, 4110–4116.

[6] a) Y. Wang and I. A. Weinstock, *Chem. Soc. Rev.* **2012**, *41*, 7479–7496; b) U. Jameel, M. Zhu, X. Chen and Z. Tong, *J. Mater. Sci.* **2016**, *51*, 2181–2198; (c) Y. Wang, A. Neyman, E. Arkhangelsky, V. Gitis, L. Meshi and I. A. Weinstock, *J. Am. Chem. Soc.* **2009**, *131*, 17412–17422; d) M. Zhang, J. Hao, A. Neyman, Y. Wang and I. A. Weinstock, *Inorg. Chem.* **2017**, *56*, 2400−2408; e) Y. Wang, O. Zeiri, M. Raula, B. L. Ouay, F. Stellacci and I. A. Weinstock, *Nat. Nanotechnol.* **2017**, *12*, 170-177; f) Y. Wang, M. Raula, Y. Wang, O. Zeiri, S. Chakraborty, G. Gan-Or, E. Gadot and I. A. Weinstock, *Angew. Chem. Int. Ed.* **2017**, *56*, 7083 –7087; g) A. Z. Ernst, L. Sun, K. Wiaderek, A. Kolary, S. Zoladek, P. J. Kulesza and J. A. Cox, *Electroanalysis* **2007**, *19*, 2103–2109; h) S. Li, X. Yu, G. Zhang, Y. Ma, J. Yao, B. Keita, N. Louis and H. Zhao, *J. Mater. Chem.* **2011**, *21*, 2282–2287; i) R. Liu, S. Li, X. Yu, G. Zhang, S. Zhang, J. Yao, B. Keita, L. Nadjo and L. Zhi, *Small* **2012**, *8,* 1398–1406.

[7] a) A. Dolbecq, E. Dumas, C. R. Mayer and P. Mialane, *Chem. Rev.* **2010**, *110*, 6009-6048; b) A. Proust, B. Matt, R. Villanneau, G. Guillemot, P. Gouzerh and G. Izzet, *Chem. Soc. Rev.* **2012**, *41*, 7605-7622; c) A. V. Anyushin, A. Kondinski and T. N. Parac-Vogt, *Chem. Soc. Rev.* **2020**, *49*, 382-432.

[8] a) J. M. Cameron, S. Fujimoto, K. Kastner, R.-J. Wei, D. Robinson, V. Sans, G. N. Newton and H. Oshio, *Chem. Eur. J.* **2017**, *23*, 47-50; b) S. Fujimoto, J. M. Cameron, R.-J. Wei, K. Kastner, D. Robinson, V. Sans, G. N. Newton and H. Oshio, *Inorg. Chem.* **2017**, *56*, 12169-12177.

[9] a) M. Piot, B. Abécassis, D. Brouri, C. Troufflard, A. Proust and G. Izzet, *Proc. Nat. Acad. Sci.* **2018**, *115*, 8895–8900; b) E. Hampson, J. M. Cameron, S. Amin, J. Kyo, J. A. Watts, H. Oshio and G. N. Newton, *Angew. Chem. Int. Ed.* **2019**, *58*, 18281–18285.

[10] S. Amin, J. M. Cameron, J. A. Watts, D. A. Walsh, V. Sans and G. N. Newton, *Mol. Syst. Des. Eng.* **2019**, *4*, 995–999.

[11] A. Klaiber, T. Kollek, S. Cardinal, N. Hug, M. Drechsler and S. Polarz, *Adv. Mater. Interfaces* **2018**, *5*, 1701430.

[12] a) C. R. Mayer, S. Neveu and V. Cabuil, *Angew. Chem. Int. Ed.* **2002**, *41*, 501-503; b) S. Hegde, S. Joshi, T. Mukherjee and S. Kapoor, *Mater. Sci. Eng. C* **2013**, *33*, 2332–2337.

[13] S. Sutter, B. Trepka, S. Siroky, K. Hagedorn, S. Theiß, P. Baum and S. Polarz, *ACS Appl. Mater. Interfaces* **2019**, *11*, 15936–15944.

[14] K. Kastner, A. J. Kibler, E. Karjalainen, J. A. Fernandes, V. Sans and G. N. Newton, *J. Mater. Chem. A* **2017**, *5*, 11577.

[15] L. E. Briand, G. T. Baronetti and H. J. Thomas, *Appl. Catal. A* **2003**, *256*, 37–50.

[16] J. -W. Park and J. S. Shumaker-Parry, *J. Am. Chem. Soc.* **2014**, *136*, 1907–1921.

[17] J. Piella, N. G. Bastus and V. Puntes, *Chem. Mater.* **2016**, *28*, 1066−1075.

[18] Z. Zheng, B. Huang, X. Qin, X. Zhang, Y. Daib and M.-H. Whangboc, *J. Mater. Chem.* **2011**, *21*, 9079–9087.

10.1002/anie.202005629

[19] a) M.-C. Bourg, A. Badia and R. B. Lennox, *J. Phys. Chem. B*, **2000**, 104, 6562-6567; b) F. Bensebaa, Y. Zhou, Y. Deslandes, E. Kruus and T. H. Ellis, *Surf. Sci.,* **1998**, 405, L472-L476.

[20] C. Fleming, D.-L. Long, N. McMillan, J. Johnston, N. Bovet, V. Dhanak, N. Gadegaard, P. Kogerler, L. Cronin and M. Kadodwala, *Nat. Nanotechnol.*, **2008**, *3*, 229-233.

[21] S. Yamazoe, Y. Hitomi, T. Shishido and T. Tanaka, *J. Phys. Chem. C* **2008**, *112*, 6869-6879.

[22] (a) V. De Waele, O. Poizat, M. Fagnoni, A. Bagno and D. Ravelli*, ACS Catal.* **2016**, *6*, 7174–7182. *(b)* C. Clavero, *Nature Photon.* **2014**, *8*, 95-103.

[23] a) J. M. Cameron, D. J. Wales and G. N. Newton, *Dalton Trans.* **2018**, *47*, 5120–5136; b) K. Suzuki, N. Mizuno and K. Yamaguchi, *ACS Catal.* **2018**, *8*, 10809-10825.

10.1002/anie.202005629

WILEY-VCH

Entry for the Table of Contents (Please choose one layout)

Layout 1:

COMMUNICATION

A new material based on gold nanoparticles stabilised by organic-inorganic hybrid polyoxometalates is described. The new nanomaterial exhibits unprecedented stability and photoactivity under visible light and can be reversibly reduced and oxidised at electrode surfaces, making it very promising for future photonic and electrochemical systems.

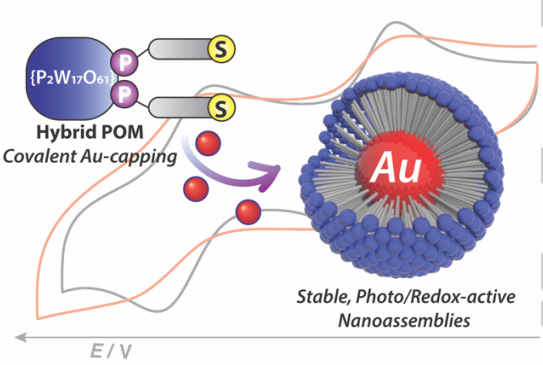

Carmen Martin, Katharina Kastner, Jamie M. Cameron, Elizabeth Hampson, Jesum Alves Fernandes Emma K. Gibson, Darren A, Walsh, Victor Sans,* and Graham N. Newton**

Page No. – Page No.

Redox-active hybrid polyoxometalate-stabilised Au nanoparticles